

# Density Contrast SPH Interfaces

B. Solenthaler and R. Pajarola

Visualization and MultiMedia Lab, University of Zurich, Switzerland

---

## Abstract

*To simulate multiple fluids realistically many important interaction effects have to be captured accurately. Smoothed Particle Hydrodynamics (SPH) has shown to be a simple, yet flexible method to cope with many fluid simulation problems in a robust way. Unfortunately, the results obtained when using SPH to simulate miscible fluids are severely affected, especially if density ratios become large. The undesirable effects reach from unphysical density and pressure variations to spurious and unnatural interface tensions, as well as severe numerical instabilities. In this work, we present a formulation based on SPH which can handle density discontinuities at interfaces between multiple fluids correctly without increasing the computational costs compared to standard SPH. The basic idea is to replace the density computation in SPH by a measure of particle densities and consequently derive new formulations for pressure and viscous forces. The new method enables the user to select the desired amount of interface tension according to the simulation problem at hand. We succeed to stably simulate multiple fluids with high density contrasts without the above described artifacts apparent in standard SPH simulations.*

---

Categories and Subject Descriptors (according to ACM CCS): I.3.5 [Computational Geometry and Object Modeling]: – Physically Based Modeling

## 1. Introduction

When simulating fluids, it is important to capture interaction effects accurately in order to reproduce real world behavior. Focusing on the interaction between multiple fluids, the challenges are to realistically model miscible as well as immiscible liquids. In that context, we can observe that surface tension forces produce effects observable in everyday life. Some examples are the formation of drops, puddles on a surface, soap bubbles, and separation of dissimilar liquids such as oil and water.

So far, multiple fluids have been modeled using Eulerian as well as Lagrangian simulations. Although the strength of grid-based methods are the smooth and visually appealing surfaces, difficulties still exist in resolving small-scale features on or below the scale of the underlying grid. It is also clear that these methods still demand more attention to avoid the severe volume loss encountered, especially when simulating several turbulent liquids [LSSF06, LTKF08]. Another approach is to use a fully particle-based fluid model such as SPH (Smoothed Particle Hydrodynamics) where particles

with different physical quantities are used to represent several fluids [MSKG05]. In contrast to level set methods, particle simulations need some effort to achieve smooth surfaces from the particles, but small-scale features down to single droplets are modeled implicitly, facilitating and enriching the simulation of complex interactions between multiple liquids.

In SPH, particles have a spatial distance (smoothing length) over which their properties are smoothed by a kernel function. Problems arise when rest densities and masses of neighboring particles vary within the smoothing length, as in such cases the smoothed quantities of a particle show falsified values. Such problems can be observed near the interface of multiple fluids with density contrasts. The erroneous quantities lead to undesirable effects, reaching from unphysical density and pressure variations to spurious and unnatural interface tensions (see for example the left image in Figure 2), and even to severe numerical instabilities.

In literature, these problems have been mainly described in computational physics so far, nevertheless, graphics applications have to cope with similar difficulties. In [Hoo98], the spurious interface tension due to degraded densities and pressures near interfaces has been described for the first time. A similar observation was reported in [AMS\*06],

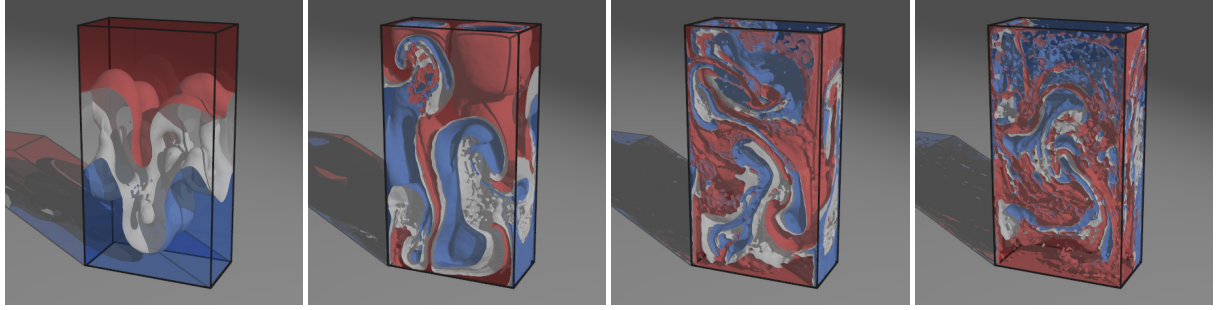


**Figure 1:** Rayleigh-Taylor instability of three fluids with density contrasts simulated with our method using one million particles. The margins are slightly cut to see the interior of the fluid. In contrast to our method, standard SPH fails to stably simulate this example.

where it has been shown that the erroneous pressure forces lead to a gap between two fluids with high density contrasts preventing important instabilities such as Kelvin-Helmholtz to evolve. When increasing the density contrast of the fluids, one has additionally to cope with severe numerical instabilities. [CL02] have shown that density ratios of more than a factor of 10 between two fluids cannot be stably simulated with SPH and that decreasing the time step does not reduce or overcome this problem. Alternatively to the standard density summation, the authors evolve the density over time according to the SPH equation for continuity (convergence equation) [Mon94]. Although the use of the convergence equation allows to set the initial densities freely, similar problems are encountered as when calculating the density directly from the particle distribution [OS03].

Because of the different requirements of computational physics and computer graphics, we focus on 3D simulations and visually demonstrate how the unnatural interface tension of the standard SPH formulation behaves. Our examples highlight the fact that when using standard SPH a user has no control over the behavior of multiple fluids and that in the worst case the simulation results in instability. As one of the main issues in graphics is to have full control over the simulated materials, we introduce a method which can handle interface discontinuities and eliminates the artifacts described above. Since our derived equations are simple modifications of a standard SPH solver, they are easy to implement and do not negatively affect the performance. In the following, we propose to compute the density based on the particle number density and we derive new formulations for the pressure equation, pressure forces as well as viscous forces. Additionally, a new interface tension model based on a smoothed and normalized color field is introduced, adding a fully controllable interface tension to our model. This allows us to simulate miscible as well as immiscible fluids according to the simulation problem of interest.

## 2. Previous Work

Similar to us, [OS03, TM05, HA06] handle density discontinuities at interfaces of multiple fluids. [OS03] have derived an adapted continuity equation and they have compared sound and shock wave simulation results to analytical solutions. Although the results for these specific applications are promising, our experiments have shown that the use of the standard as well as the adapted continuity equation does not produce stable results for long-term simulations. This is due to severe density integration errors, especially when using large time steps and low-order time integration schemes which is important for the targeted type of applications. Both [TM05] and [HA06] use a corrected density summation for their investigations. The former work concentrates on miscible flow in fracture apertures with complex geometry and combines a modified SPH flow equation with an advection-diffusion equation. Tension forces are not included in their model, and the pressure computation does only allow the simulation of closed systems or systems with periodic boundary conditions. The latter work focuses on the investigation of numerical examples such as droplet oscillation and deformation in shear flow in 2D and the comparison to analytical solutions. This work has been extended with an incompressibility condition in [HA07].

Besides the works already mentioned above, earlier research on multi-phase fluid simulation methods includes [KFL00, PSvdW03, HK05], addressing discontinuous properties, and [HK03, GH04, MUM\*06, ZYP06], focusing on bubbles and foam. While these techniques are all fully Eulerian, [LTKF08] introduced a level set method which is coupled with SPH particles representing diffuse regions such as spray. A shallow water simulation using SPH particles to represent foam has been presented in [TSS\*07], and a pure particle simulation based on SPH to deal with multiple liquids and boiling effects has been demonstrated in [MSKG05]. In the latter work, density ratios are kept small, reducing the visibility of the problems coming with multiple fluids. Immiscible fluids have been an-

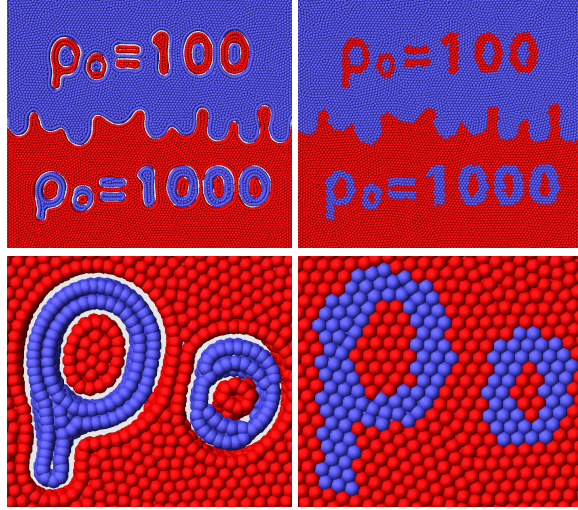


**Figure 2:** In contrast to the new method (right), the use of standard SPH produces a spurious interface tension and a gap between two fluids with a density contrast (left).

imated in [MY06] by explicitly detecting colliding particles.

### 3. Standard SPH Formulation

SPH is a Lagrangian model where the fluid is discretized by particles carrying field quantities  $A$ . At any position  $\mathbf{r}$ , these quantities can be evaluated by summing up the contributions of the neighboring particles  $j$

$$A(\mathbf{r}) = \sum_j \frac{m_j}{\rho_j} A_j W(\mathbf{r} - \mathbf{r}_j, h), \quad (1)$$

where,  $W(\mathbf{r} - \mathbf{r}_j, h)$  is the weighting kernel with smoothing length  $h$ ,  $m_j$  the mass of particle  $j$ , and  $\rho_j$  its density. Applying the SPH interpolation to the density field, we get

$$\rho_i = \sum_j m_j W(\mathbf{r}_{ij}, h), \quad (2)$$

where  $\mathbf{r}_{ij} = \mathbf{r}_i - \mathbf{r}_j$ . The pressure  $p$  of a particle is then derived from the state equation. One possibility is to use the pressure equation according to [DC96]

$$p_i = k(\rho_i - \rho_0), \quad (3)$$

where  $\rho_0$  is the rest density of the fluid, or to use the Tait equation [Bat67]

$$p_i = \frac{k\rho_0}{\gamma} \left( \left( \frac{\rho_i}{\rho_0} \right)^\gamma - 1 \right). \quad (4)$$

In the literature, the stiffness  $k$  is chosen as high as possible and  $\gamma$  is set to 7 to enforce low density variations [Mon92]. The pressure and viscous force fields are directly derived from the Navier-Stokes equations. In [MCG03, MSKG05],

these fields are computed by

$$\mathbf{F}_i^{pressure} = -\frac{m_i}{\rho_i} \sum_j \frac{m_j}{\rho_j} \frac{p_i + p_j}{2} \nabla W(\mathbf{r}_{ij}, h) \quad (5)$$

$$\mathbf{F}_i^{viscosity} = \frac{m_i}{\rho_i} \sum_j \frac{\mu_i + \mu_j}{2} \frac{m_j}{\rho_j} (\mathbf{v}_j - \mathbf{v}_i) \nabla^2 W(\mathbf{r}_{ij}, h), \quad (6)$$

where  $\mu$  is the viscosity constant of a particle. Alternatively to Equation 5, a pressure force equation according to [Mon92] can be used:

$$\mathbf{F}_i^{pressure} = -\sum_j m_i m_j \left( \frac{p_i}{\rho_i^2} + \frac{p_j}{\rho_j^2} \right) \nabla W(\mathbf{r}_{ij}, h). \quad (7)$$

For all equations, we have chosen the weighting kernels to be as introduced by the authors in their original papers.

## 4. Adapted SPH Equations for Miscible Fluids

### 4.1. Problem Description

The standard SPH density summation (Equation 2) becomes problematic as soon as a particle has neighboring particles with different rest densities (and therefore different masses, as we require constant rest volumes throughout the particles). This is the case close to the interface of two fluids with a rest density contrast. For particles close to the interface, the computed density is underestimated if they belong to the fluid with higher rest density, and overestimated otherwise. This happens because the standard SPH formulation smoothes the density and cannot accurately represent sharp density changes as it would be desired. This is illustrated in Figure 3 (a) and (b) and visualized in the left part of Figure 4. The falsified densities induce wrong pressure values close to the interface (Figure 3 (c)), leading to a spurious interface tension and a large gap between the fluids (Figure 2). Even worse, the erroneous pressure forces induce numerical instabilities at the interface and make it impossible to simulate multiple fluids with high density ratios.

### 4.2. Comparison of Pressure Force Equations

Regarding the standard SPH formulation for multiple different fluids, not only the density is problematic but also the computation of the pressure forces. We compare the two techniques mainly used in graphics, which are Equation 5 and Equation 7, and derive adapted equations applicable to multiple fluids later on.

Our experiments have shown that for fluids with small density contrasts (density ratios of approximately a factor of 2), both pressure force equations result in almost the same behavior regarding spurious interface tension and the undesired gap between the fluids. When increasing the density contrast, the use of Equation 5 leads to unstable simulations which cannot be overcome even by decreasing the time step of the simulation significantly (Figure 5 (a) upper-left). For these tests, we used a viscosity coefficient  $\mu$  of  $5\text{Ns/m}^2$  and

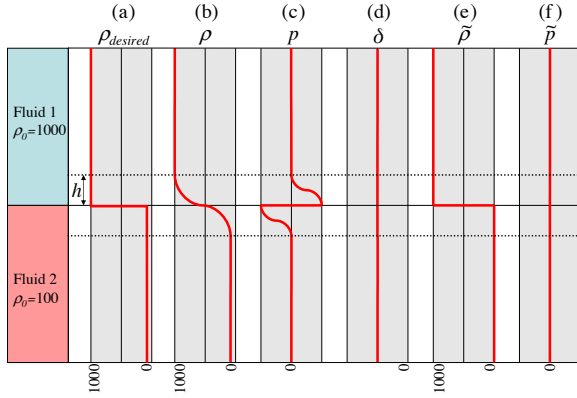


**Figure 3:** Several physical quantities in a 1D example. Standard SPH cannot represent actual desired density discontinuities (a), as it smoothes the density over the interface (b). As a result, erroneous pressures are present near the interface (c). We derive new SPH equations using the particle density (d), resulting in densities (e) and pressures (f) with the desired behavior.

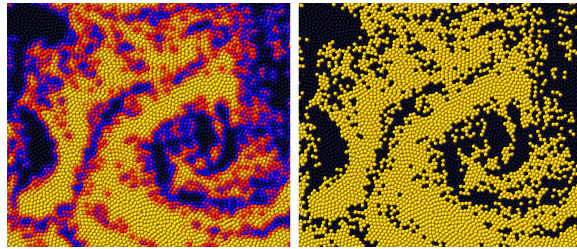


**Figure 4:** Standard SPH density (left) versus our corrected density (right). The two fluids have rest densities of  $1000 \text{ kg/m}^3$  and  $100 \text{ kg/m}^3$ . The computed density is color-coded with yellow being  $1000$ , red  $700$ , blue  $400$ , and black  $100$ , respectively.

a stiffness  $k$  of  $1000 \text{ Nm/kg}$ . When using the parameters described in [MSKG05] which are a  $\mu$  of  $20 \text{ Ns/m}^2$  and a  $k$  of  $20 \text{ Nm/kg}$ , the simulation of density ratios up to a factor of 10 is feasible, but it comes at the expense of undesired smoothing and compressibility effects. The simulation behaves differently when using Equation 7 as it is stable up to a density ratio of 10 (Figure 5 (a) lower-left). Larger density contrasts are not stable, and reducing the time step has again no effect onto the stability.

In Section 4.4, we present the adapted equations for both pressure force equations and we show that the numerical instabilities and spurious interface tensions are eliminated for both approaches (Figure 5 (b)).

### 4.3. Density Model

To handle density discontinuities at interfaces between multiple fluids with varying rest densities correctly, we propose to replace the standard density summation given by Equation 2 by a measure of particle density (sometimes called number density), similar to [OS03, PTB\*03, TM05, HA06]. The idea is to make each particle treat its neighbors as if they would have the same rest density and mass as itself. The particle density  $\delta_i$  of a particle is defined as

$$\delta_i = \sum_j W(\mathbf{r}_{ij}, h). \quad (8)$$

We compute the adapted density  $\tilde{\rho}_i$  of a particle by multiplying the particle density by the mass of the particle

$$\tilde{\rho}_i = m_i \delta_i = m_i \sum_j W(\mathbf{r}_{ij}, h). \quad (9)$$

For the volume  $V$  of a particle we then get

$$V_i = \frac{m_i}{\tilde{\rho}_i} = \frac{1}{\delta_i}. \quad (10)$$

For a single fluid where all particles have equal masses and rest densities, the presented formulation corresponds exactly to the standard SPH formulation. But when dealing with multiple fluids of different densities we can achieve a density field reproducing sharp density changes at the interface of the fluids as shown in Figure 4 on the right.

### 4.4. Adapted Pressure and Pressure Forces

Following [Bat67, Mon94], we use the Tait equation (Equation 4) to compute the pressure. In this formula, we replace the standard SPH density  $\rho$  by the adapted density  $\tilde{\rho}$  introduced above, yielding the following equation for the pressure  $\tilde{p}$

$$\tilde{p}_i = \frac{k \rho_0}{\gamma} \left( \left( \frac{\tilde{\rho}_i}{\rho_0} \right)^\gamma - 1 \right). \quad (11)$$

Consequently, we can derive a new formulation for the pressure force. In the pressure gradient term  $a = -\nabla p/\rho$  of the Navier Stokes equations we replace  $\rho$  by  $\tilde{\rho}$  and  $p$  by  $\tilde{p}$ , yielding

$$a = -\frac{\nabla \tilde{p}}{\delta m}. \quad (12)$$

For the pressure force  $\mathbf{F}^{pressure} = ma$  we then get

$$\mathbf{F}^{pressure} = -\frac{\nabla \tilde{p}}{\delta}. \quad (13)$$

When using the formulation of [MCG03], the pressure force is derived by applying the SPH rules to  $\nabla p$  and symmetrizing the equation. In the standard approach, this yields Equation 5. We derive the adapted pressure force equation similarly, but we again replace  $\rho$  by  $\tilde{\rho}$  and  $p$  by  $\tilde{p}$ , yielding the final equation for the pressure force

$$\mathbf{F}_i^{pressure} = -\frac{1}{\delta_i} \sum_j \frac{1}{\delta_j} \frac{\tilde{p}_i + \tilde{p}_j}{2} \nabla W(\mathbf{r}_{ij}, h). \quad (14)$$

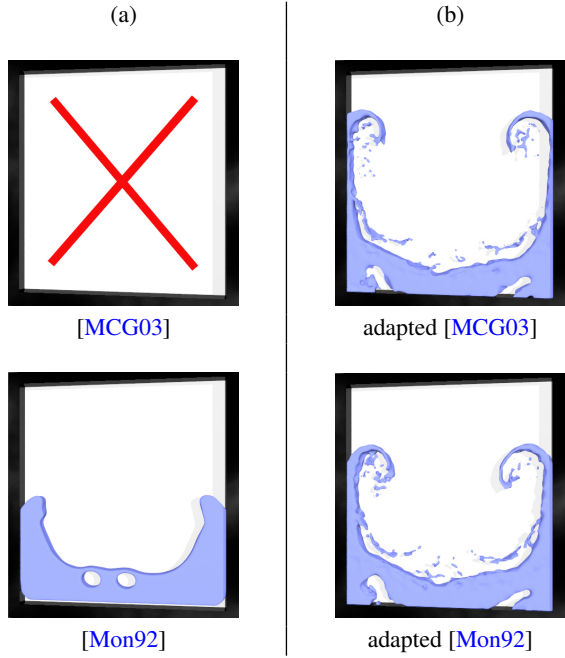


**Figure 5:** Two fluids with a density ratio of 10 are simulated with two different pressure force equations, (a) on the left using the original formulations, and (b) on the right using our adapted equations. While the standard formulations result in instability (upper left: Equation 5) and spurious tension problems (lower left: Equation 7), these problems can be overcome by using our modified equations (Equation 14 and Equation 19).

Monaghan's pressure force equation [Mon92] is derived differently from the one in [MCG03]. In Monaghan's derivation, the pressure gradient term of the Navier-Stokes equations is symmetrized by applying the quotient rule

$$\frac{\nabla p}{\rho} = \nabla \left( \frac{p}{\rho} \right) + \frac{p}{\rho^2} \nabla \rho. \quad (15)$$

This formulation uses the density gradient  $\nabla \rho$  which is problematic when applying our modified density  $\tilde{\rho}$  for multiple fluids. In contrast to the standard SPH density  $\rho$  which was smoothed over the interface (Figure 3 (b)),  $\tilde{\rho}$  is discontinuous (Figure 3 (e)) and the derivative thereof is thus not defined. Simply inserting  $\tilde{\rho}$  and  $\tilde{\rho}$  into Monaghan's pressure force equation results in severe instabilities at the interface.

To solve this problem, we have to derive the pressure gradient in a different way. Our approach is to replace the discontinuous quantity  $\nabla \rho$  by a  $C^1$  continuous one. We use Equation 13 and apply the quotient rule. Thus, Equation 15 becomes

$$\frac{\nabla \tilde{\rho}}{\delta} = \nabla \left( \frac{\tilde{\rho}}{\delta} \right) + \frac{\tilde{\rho}}{\delta^2} \nabla \delta. \quad (16)$$

As can be seen, the discontinuous quantity  $\nabla \rho$  is replaced

by the continuous and derivable particle density (Figure 3 (d)). Applying the SPH rules, Equation 16 can be rewritten to

$$\frac{\nabla \tilde{\rho}}{\delta} = \sum_j \left( \frac{\tilde{\rho}_j}{\delta_j} + \frac{\tilde{\rho}_i}{\delta_i^2} \delta_j \right) V_j \nabla W(\mathbf{r}_{ij}, h). \quad (17)$$

In Equation 17, the volume  $V_j$  can be replaced by  $1/\delta_j$ , resulting in

$$\frac{\nabla \tilde{\rho}}{\delta} = \sum_j \left( \frac{\tilde{\rho}_j}{\delta_j^2} + \frac{\tilde{\rho}_i}{\delta_i^2} \right) \nabla W(\mathbf{r}_{ij}, h). \quad (18)$$

Finally, we get for the pressure force of a particle  $i$

$$\mathbf{F}_i^{pressure} = - \sum_j \left( \frac{\tilde{\rho}_j}{\delta_j^2} + \frac{\tilde{\rho}_i}{\delta_i^2} \right) \nabla W(\mathbf{r}_{ij}, h). \quad (19)$$

In [TM05, HA06], this formulation has been derived differently but adopted in a similar way.

#### 4.5. Adapted Viscous Forces

We derive the adapted viscous forces by replacing the density  $\rho$  by the modified density  $\tilde{\rho}$  in the viscosity term  $\mu \nabla^2 \mathbf{v} / \rho$  of the Navier-Stokes equations as well as in the derived SPH formulation. We end up with the following equation for the viscous force

$$\mathbf{F}_i^{viscosity} = \frac{1}{\delta_i} \sum_j \frac{\mu_i + \mu_j}{2} \frac{1}{\delta_j} (\mathbf{v}_j - \mathbf{v}_i) \nabla^2 W(\mathbf{r}_{ij}, h). \quad (20)$$

#### 4.6. Controlling Interface Tension Forces

With the modified density, pressure, and force equations presented in the last sections we are able to eliminate all spurious and unnatural interface tension effects which are present when using the standard SPH method. Now we can introduce a fully controllable interface tension to our model, enabling a user to select the desired amount according to the simulation problem of interest.

Similar to [Mor00], we use a color field to model tension forces. In contrast to their work and to [MSKG05, HA06], we model the tension forces such that the free surface remains unaffected while the desired interface tension between any two different fluids can be controlled arbitrarily. If desired by the user, additional tension forces acting at the free surface can be simply added by using the technique presented in [Mor00]. We define the interface tension force to be

$$\mathbf{F}^{interface} = \frac{1}{\delta_i} \sigma \kappa \mathbf{n}, \quad (21)$$

where  $\sigma$  is the tension coefficient defining the strength of the force and  $\mathbf{n}$  is the normal on the interface. This force acts to smooth interface regions of high curvature  $\kappa$ , in an attempt to minimize the total surface area. In order to compute  $\mathbf{n}$  and  $\kappa$ , a color field is defined which is non-zero at all particle locations, and different color values are assigned to different fluid types. As suggested in [Mor00], we smooth the color

field to obtain more accurate estimates of the normals  $\mathbf{n} = \nabla c$  afterwards. In order to avoid tensions at the free surface, we additionally normalize the smoothed color value. Thus, the smoothed color value is given by

$$\langle c \rangle_i = \frac{\sum_j \frac{1}{\delta_j} c_j W(\mathbf{r}_{ij}, h)}{\sum_j \frac{1}{\delta_j} W(\mathbf{r}_{ij}, h)}. \quad (22)$$

The accuracy of the normal can be improved additionally by using the difference between neighboring particle colors

$$\mathbf{n}_i = \sum_j \frac{1}{\delta_j} (\langle c \rangle_j - \langle c \rangle_i) \nabla W(\mathbf{r}_{ij}, h). \quad (23)$$

The curvature, which is defined as  $\kappa = -\nabla \cdot \hat{\mathbf{n}}$ , where  $\hat{\mathbf{n}}$  is the unit normal, can be formulated with SPH and our adapted density as

$$\kappa = \frac{-\sum_j \frac{1}{\delta_j} (\hat{\mathbf{n}}_j - \hat{\mathbf{n}}_i) \cdot \nabla W(\mathbf{r}_{ij}, h)}{\sum_j \frac{1}{\delta_j} W(\mathbf{r}_{ij}, h)}. \quad (24)$$

## 5. Results and Discussion

To demonstrate the effectiveness of our approach, we simulated several examples with varying resolution ranging from 20k to 1M particles on an Intel Core2 2.66 GHz. The computational cost for the examples range from 0.2s to 10s per time step and 20s to 40min to render one frame using the raytracing approach presented in [SSP07]. If not mentioned differently, we used Equation 19 to compute the pressure forces. For all scenes, we used the leapfrog time integration scheme with constant time step size throughout the simulation. The time step size was initially determined by using a CFL condition [CFL67]. In our examples, this value was dominated by the stiffness of the fluid and was between 10e-3s and 10e-4s. Note that, compared to standard SPH, the time step size does not have to be decreased when using our method, and the cost per time step stays the same. Furthermore, our approach makes the simulation of high density ratios possible which cannot be stably simulated with standard SPH. An example where standard SPH failed in our tests is depicted in Figure 1, where 1 million particles representing 3 different fluids with a density ratio of 20 in total were simulated with our method. The margins are slightly cut to see the interior of the fluid.

Figure 6 depicts another Rayleigh-Taylor instability with 80k particles representing two fluids with a density ratio of 10. Although we were able to simulate this example using Monaghan's pressure equation, the result is suffering from severe and unnatural interface tension (Figure 6 (a), Figure 2). Our modifications eliminate the spurious interface tension effects (Figure 6 (b)), and allows us to explicitly add tension forces with full control over its strength (Figure 6 (c), (d)), facilitating the simulation of miscible and immiscible fluids.

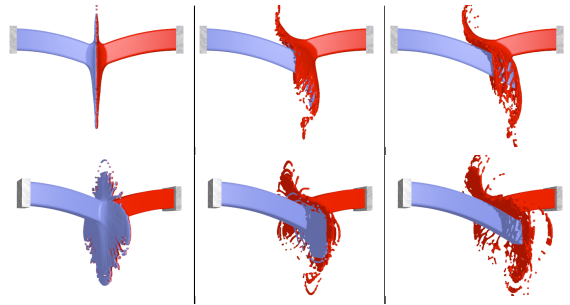


**Figure 7:** From left to right: two fluids with a density ratio of 1, 10, and 100, respectively.

In the last sections, we derived new equations for two different types of pressure force equations which are often used in graphics, allowing a user to select the desired formulation. Regardless of the type, the instability and spurious tension problems of the standard formulation (Figure 5, (a)) can be overcome by using our new method (Figure 5, (b)). While the standard SPH technique allows only the simulation of density ratios up to 2 or 10, respectively (depending on the type of pressure force equation as we have discussed in Section 4.2), our method enables the simulation of fluids with very high density ratios without having stability problems. This is demonstrated in Figure 7, where fluids with density ratios of up to 100 were simulated.

Although our method overcomes the discontinuity problems at interfaces of multiple fluids, we would like to point out that other limitations of SPH remain. When dealing with large density ratios in SPH, the behavior of small, light volumes is negatively affected as the buoyancy is damped in specific situations. Although viscosity dampens turbulence and buoyancy to some extent, we have observed that this defect is apparent even without integrating any viscosity into the SPH model. We believe that this defect results from pressure forces compelling the particles to arrange in a stable equilibrium lattice structure [LSRS99] (this crystallization effect is strongly visible in Figure 2). As a result, the buoyant volumes have to break open the crystallized particle configuration in order to rise. Thus the buoyancy may get weakened, most notably visible at small volumes and when the system comes to rest. Although this effect will need some attention in the future, it is not in the scope of this paper which focuses on the specific challenge of spurious and unphysical interface tension effects with the standard SPH approach. Our proposed solution addresses this identified problem in such a way that no other aspects of SPH are seriously affected, being it its simulation performance or its advantages in modeling small-scale features and multiple materials, but also for that matter other disadvantages remain.

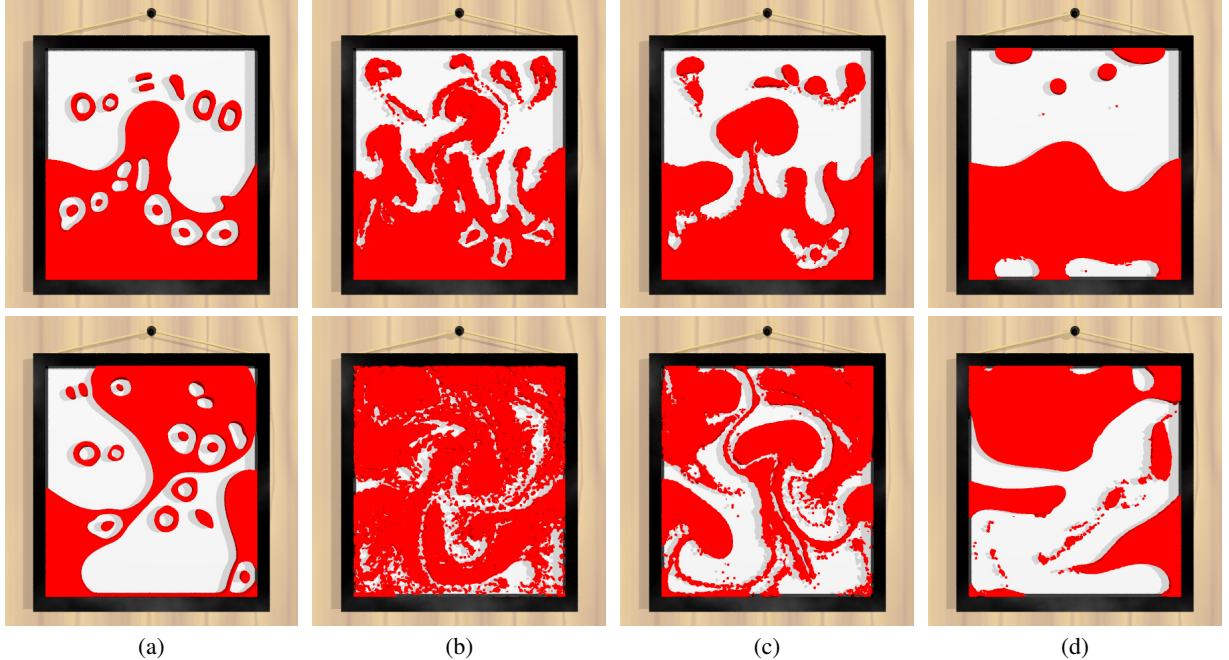


**Figure 6:** Two fluids with a density ratio of 10 at two different points in time. While standard SPH produces unnatural interface tension (a), our method prevents any spurious tension between the fluids (b). As a result, interface tension forces can be added with full control, (c) and (d) show a tension strength of  $\sigma = 5$  and  $\sigma = 35$ , respectively.

## 6. Conclusion

Our modifications of the SPH formulation corrects for density problems, spurious and unphysical interface tension, and instabilities otherwise present at high density contrast interfaces. High density ratios can now be simulated stably, and the fluid behavior can be controlled according to the simulation problem of interest. The modification is easy to implement and does not require smaller time steps than the original method.

## References

- [AMS\*06] AGERTZ O., MOORE B., STADEL J., POTTER D., MINIATI F., READ J., MAYER L., GAWRYSZCZAK A., KRAVTSOV A., MONAGHAN J., NORDLUND A., PEARCE F., QUILIS V., RUDD D., SPRINGEL V., STONE J., TASKER E., TEYSSIER R., WADSLEY J., WALDER R.: Fundamental differences between sph and grid methods. *Mon. Not. R. astr. Soc. astro-ph/0610051* (2006).
- [Bat67] BATCHELOR G.: *An introduction to fluid dynamics*. Cambridge University Press, 1967.
- [CFL67] COURANT R., FRIEDRICH K., LEWY H.: On the partial difference equations of mathematical physics. *IBM J. 11* (1967), 215–234.
- [CL02] COLAGROSSI A., LANDRINI M.: Numerical simulation of interfacial flows by smoothed particle hydrodynamics. *Comput. Phys. 191* (2002), 448–475.
- [DC96] DESBRUN M., CANI M.-P.: Smoothed particles: A new paradigm for animating highly deformable bodies. In *Eurographics Workshop on Computer Animation and Simulation* (1996), pp. 61–76.
- [GH04] GREENWOOD S. T., HOUSE D. H.: Better with bubbles: enhancing the visual realism of simulated fluid. In *Symposium on Computer Animation* (2004), pp. 287–296.
- [HA06] HU X. Y., ADAMS N. A.: A multi-phase sph method for macroscopic and mesoscopic flows. *Comput. Phys. 213*, 2 (2006), 844–861.
- [HA07] HU X. Y., ADAMS N. A.: An incompressible multi-phase sph method. *J. Comput. Phys. 227*, 1 (2007), 264–278.
- [HK03] HONG J. M., KIM C. H.: Animation of bubbles in liquid. *Computer Graphics Forum 22*, 3 (2003), 253–262.
- [HK05] HONG J. M., KIM C. H.: Discontinuous fluids. *ACM Trans. Graph. (SIGGRAPH Proc.) 24*, 3 (2005), 915–920.
- [Hoo98] HOOVER W.: Isomorphism linking smooth particles and embedded atoms. *Physics A 260* (1998), 244–254.

- [KFL00] KANG M., FEDKIW R. P., LIU X.-D.: A boundary condition capturing method for multiphase incompressible flow. *J. Sci. Comput.* 15, 3 (2000), 323–360.
- [LSRS99] LOMBARDI J. C., SILLS A., RASIO F. A., SHAPIRO S. L.: Tests of spurious transport in smoothed particle hydrodynamics. *J. Comput. Phys.* 152, 2 (1999), 687–735.
- [LSSF06] LOSASSO F., SHINAR T., SELLE A., FEDKIW R.: Multiple interacting liquids. *ACM Trans. Graph. (SIGGRAPH Proc.)* 25, 3 (2006), 812–819.
- [LTKF08] LOSASSO F., TALTON J., KWATRA J., FEDKIW R.: Two-way coupled sph and particle level set fluid simulation. *IEEE TVCG* (2008), in press.
- [MCG03] MÜLLER M., CHARYPAR D., GROSS M.: Particle-based fluid simulation for interactive applications. In *Symposium on Computer Animation* (2003), pp. 154–159.
- [Mon92] MONAGHAN J.: Smoothed particle hydrodynamics. *Annu. Rev. Astron. Physics* 30 (1992), 543.
- [Mon94] MONAGHAN J.: Simulating free surface flows with sph. *Comput. Phys.* 110 (1994), 399–406.
- [Mor00] MORRIS J. P.: Simulating surface tension with smoothed particle hydrodynamics. *International Journal for Numerical Methods in Fluids* 33 (2000), 333–353.
- [MSKG05] MÜLLER M., SOLENTHALER B., KEISER R., GROSS M.: Particle-based fluid-fluid interaction. In *Symposium on Computer Animation* (2005), pp. 237–244.
- [MUM\*06] MIHALEF V., UNLUSU B., METAXAS D., SUSSMAN M., HUSSAINI M. Y.: Physics based boiling simulation. In *Symposium on Computer Animation* (2006), pp. 317–324.
- [MY06] MAO H., YANG Y.-H.: Particle-based immiscible fluid-fluid collision. In *GI '06: Proceedings of Graphics Interface 2006* (2006), pp. 49–55.
- [OS03] OTT F., SCHNETTER E.: A modified sph approach for fluids with large density differences, 2003.
- [PSvdW03] PELUPESSY F. I., SCHAAP W. E., VAN DE WEYGAERT R.: Density estimators in particle hydrodynamics: Dtfe versus regular sph. *Astronomy and Astrophysics* 403 (2003), 389–398.
- [PTB\*03] PREMOZE S., TASDIZEN T., BIGLER J., LEFOHN A., WHITAKER R. T.: Particle-based simulation of fluids. In *Proceedings of Eurographics* (2003), pp. 401–410.
- [SSP07] SOLENTHALER B., SCHLÄFLI J., PAJAROLA R.: A unified particle model for fluid-solid interactions. *Journal of Computer Animation and Virtual Worlds* 18, 1 (2007), 69–82.
- [TM05] TARTAKOVSKY A. M., MEAKIN P.: A smoothed particle hydrodynamics model for miscible flow in three-dimensional fractures and the two-dimensional rayleigh-taylor instability. *Comput. Phys.* 207, 2 (2005), 610–624.
- [TSS\*07] THÜREY N., SADLO F., SCHIRM S., MÜLLER-FISCHER M., GROSS M.: Real-time simulations of bubbles and foam within a shallow water framework. In *Symposium on Computer Animation* (2007), pp. 191–198.
- [ZYP06] ZHENG W., YONG J.-H., PAUL J.-C.: Simulation of bubbles. In *Symposium on Computer Animation* (2006), pp. 325–333.